

Study on Electro Optic Characteristics of In-plane Switching Mode Liquid Crystal Display using Transparent Electrode

Il Sub Song^a, In-Su Baik^{**a}, Tae Man Kim^a, Seung Hee Lee^{*a}, Do Sung Kim^b, Hoe-Sub Soh^{*b}, and Woo Yeol Kim^b

Abstract

Voltage-dependent transmittance characteristics associated with various cell parameters have been studied in-plane switching liquid crystal display when both common and pixel electrodes are transparent. When both electrodes are opaque, the transmittance is related to only the distance (l) between electrodes. However, where transparent electrode is used, it is influenced not only the l but also an electrode width (w) and rubbing angle. In addition, these factors are related to operating voltage which shows maximal transmittance. To maximize the light efficiency of the cell and obtain low operating voltage, the above-mentioned cell parameters need to be optimized.

Keywords : liquid crystal display, in-plane switching, transparent electrode

1. Introduction

Liquid crystal displays (LCDs) have areas applied in four major areas namely mobile phones, notebooks, monitors and televisions. In notebooks, wide viewing angle LC modes were not applied at first. Therefore, when the display size was less than about 17", the twisted nematic (TN) mode [1, 2] was used. However, nowadays, there is greater demand for notebooks with high image quality with high brightness. But, the TN mode has demerits such as reversal gray scales, decreases in the contrast ratio, and color shift, when the display is observed in an oblique viewing direction. In that respect, the TN mode was regarded as inadequate to realize a high image quality. To overcome the above-mentioned problems, various LC modes were proposed such as in plane switching (IPS) mode [3, 4], fringe field switching (FFS) mode [5~7], and multi-domain vertical alignment (MVA) mode [8] which exhibit excellent viewing angle characteristics. Especially, in the IPS and FFS modes, the LC director rotates almost in plane. In the IPS mode, the LC director above electrode does not rotate enough so that the low transmittance is an intrinsic problem despite the fact that transparent or opaque

electrodes are used. If the electrode width (w) is reduced and the distance (l) between electrodes is increased in order to improve the transmittance, this results in the increase in the operating voltage (V_{op}), which is not affordable in portable displays because high operating voltage increases power consumption.

In this paper, we will discuss ways to improve the transmittance with low operating voltage in the IPS mode. In the device, when opaque electrodes as common and pixel electrodes are used, the transmittance is dependent on only l . However, when transparent electrodes are used, the transmittance and V_{op} is determined by not only l but also w and the rubbing angle. Therefore, parameter optimization via defining the relationship between parameters need to be examined to improve the transmittance with low V_{op} through calculations and experiments.

2. Cell Structure and Switching Principle of IPS Mode

In the IPS mode where uniaxial LC medium exists under crossed polarizers, the normalized light transmittance is defined by

$$\eta = T/T_0 = \sin^2(2\phi) \sin^2(\pi d \Delta n / \lambda) \quad (1)$$

where ϕ is an angle between transmission axis of polarizers and optical axis of LC molecules, d is a cell gap, Δn is birefringence of the LC and λ is a wavelength of an incident light. In the device, the in-plane field drives the

Manuscript received July 29, 2004; accepted for publication September 17, 2004.

This work is supported by LG-Philips LCD.

* Members, KIDS.

Corresponding Author : Seung Hee Lee

a. School of Advanced Materials Engineering, Chonbuk National University, Chonju-si, Chonbuk 561-756, Korea.

b. Advanced Technology Development Team, LG-Philips LCD, Kumi-si, Kyungbuk, 730-726, Korea.

E-mail : ish1@chonbuk.ac.kr Tel : +63 270-2343 Fax : +63 270-2341

homogeneously aligned LCs to rotate in parallel to the substrate, giving rise to transmittance from a dark state. Fig. 1 shows off and on state of the IPS mode cell. As shown in this figure, the homogeneously aligned nematic LCs rotate in the plane with bias voltage and the LCs rotate very slightly above the electrodes, meaning that the transmittance also occurs even above electrode. Therefore, to calculate the normalized transmittance of the cell we must consider it in two areas: above electrode (η_w) and between electrodes (η_l). Thus the light intensity of the cell transmitted should be defined as follows:

$$\begin{aligned} I &= \eta_l \times l \text{ for opaque electrodes} \\ I &= \eta_w \times w + \eta_l \times l \text{ for transparent electrodes} \end{aligned} \quad (2)$$

According to Eqn. (2), the transmitted intensity of the cell when using the transparent electrode is determined by η_w , w , η_l , and l .

For calculations purposes, we used the commercially available software "LCD Master" (Shintech, Japan), where the motion of the LC director is calculated based on the Ericksen-Leslie theory and 2×2 Jones matrix is applied for optical transmittance calculation⁹⁾. The LC with physical properties ($\Delta n = 0.08$ at $\lambda = 550 \text{ nm}$, $\Delta \epsilon = + 8.2$, $K_{11} = 9.7 \text{ pN}$, $K_{22} = 5.2 \text{ pN}$, $K_{33} = 13.3 \text{ pN}$) was used. The surface tilt angle was assumed to be 2° .

3. Electro-optic Characteristics of the IPS Mode using Transparent Electrode

First, we investigated the voltage-dependent light efficiency characteristics as a function of rubbing angles

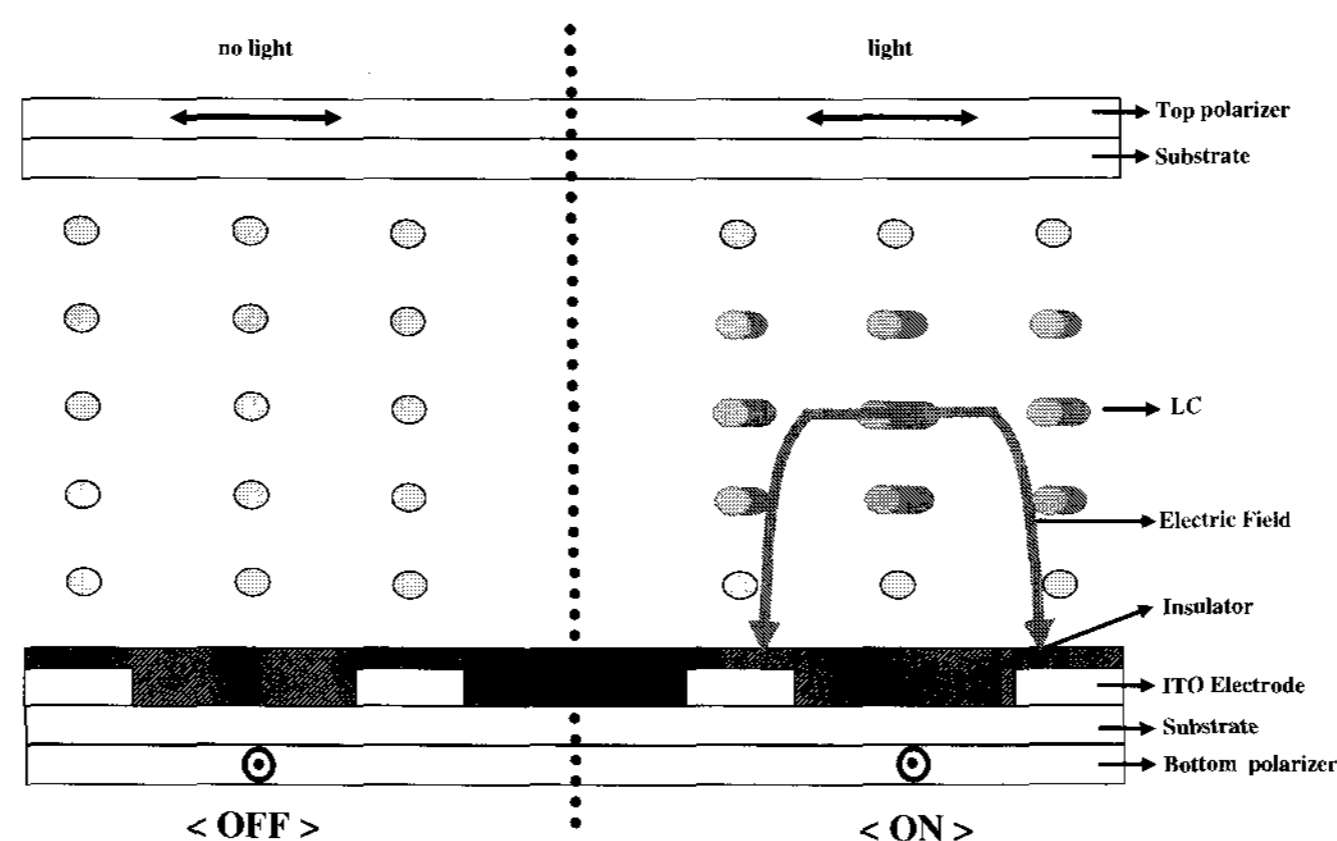


Fig. 1. Cell structure of the IPS mode in the off and on states using the LC with positive dielectric anisotropy.

with respect to in-plane field direction when using transparent electrode. Fig. 2 shows the calculated voltage dependent light efficiency with rubbing angles near the operating voltage. In this figure, the electrode width and the distance between them are $5 \mu\text{m}$ and $10 \mu\text{m}$, respectively. The cell gap is $4 \mu\text{m}$. In the IPS device with opaque electrodes, the optical transmittance is not a function of rubbing angles when it is in the range between 89° and 65° [10]. However, in the device with transparent electrodes it is clearly dependent on the rubbing angle such that η increases with increasing rubbing angle. Meanwhile, the V_{op} decreases with increasing rubbing angle. This implies that for the notebook display with low driving voltage and high transmittance, a large rubbing angle is more favorable.

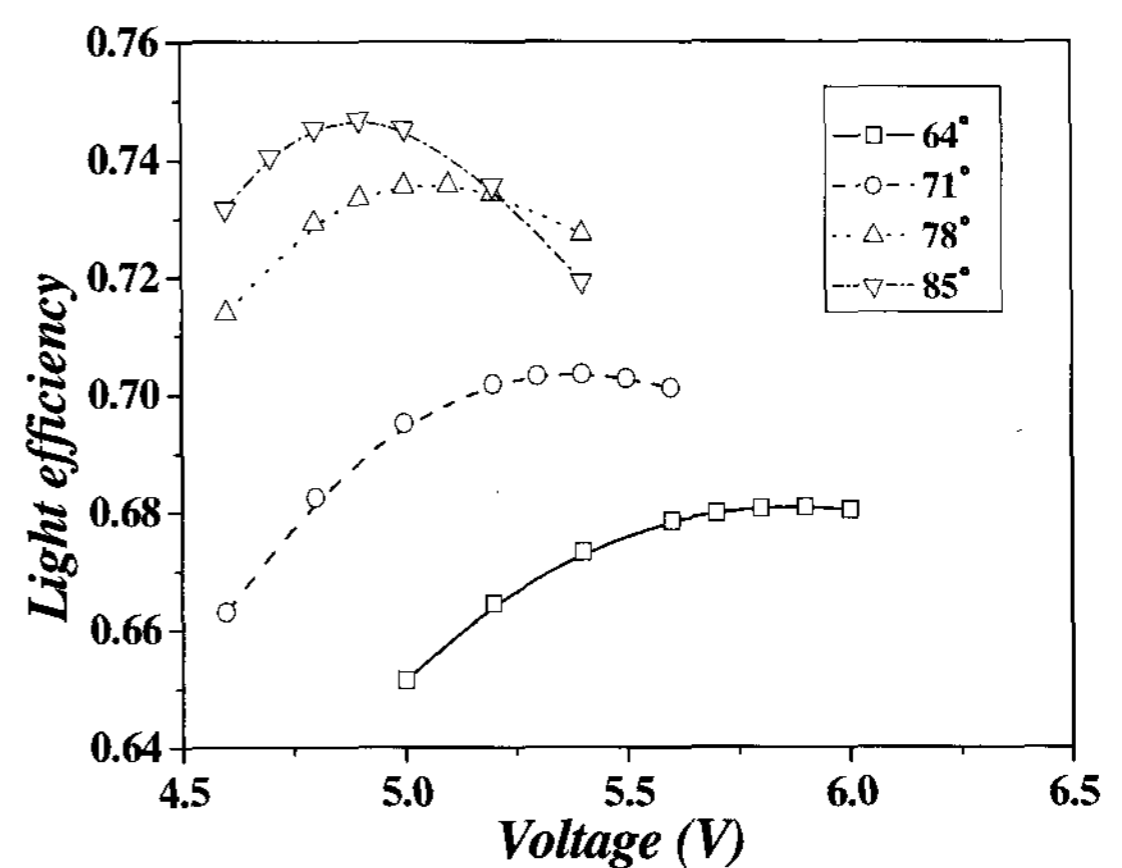


Fig. 2. Calculated voltage-dependent light efficiency for different rubbing angles.

To understand the origin of the rubbing-angle dependent η , we calculated it along the electrode position including the w and l for each rubbing angle, as

shown in Fig. 3. Interestingly, η_i is almost independent of the rubbing angle but η_w is strongly dependent on the rubbing angle. This indicates that the larger the rubbing angle, the more LCs above the electrodes become twisted, resulting in increased transmittance due to increased ϕ value. Therefore, we calculated the twist angle distribution at three different positions above the electrode for each

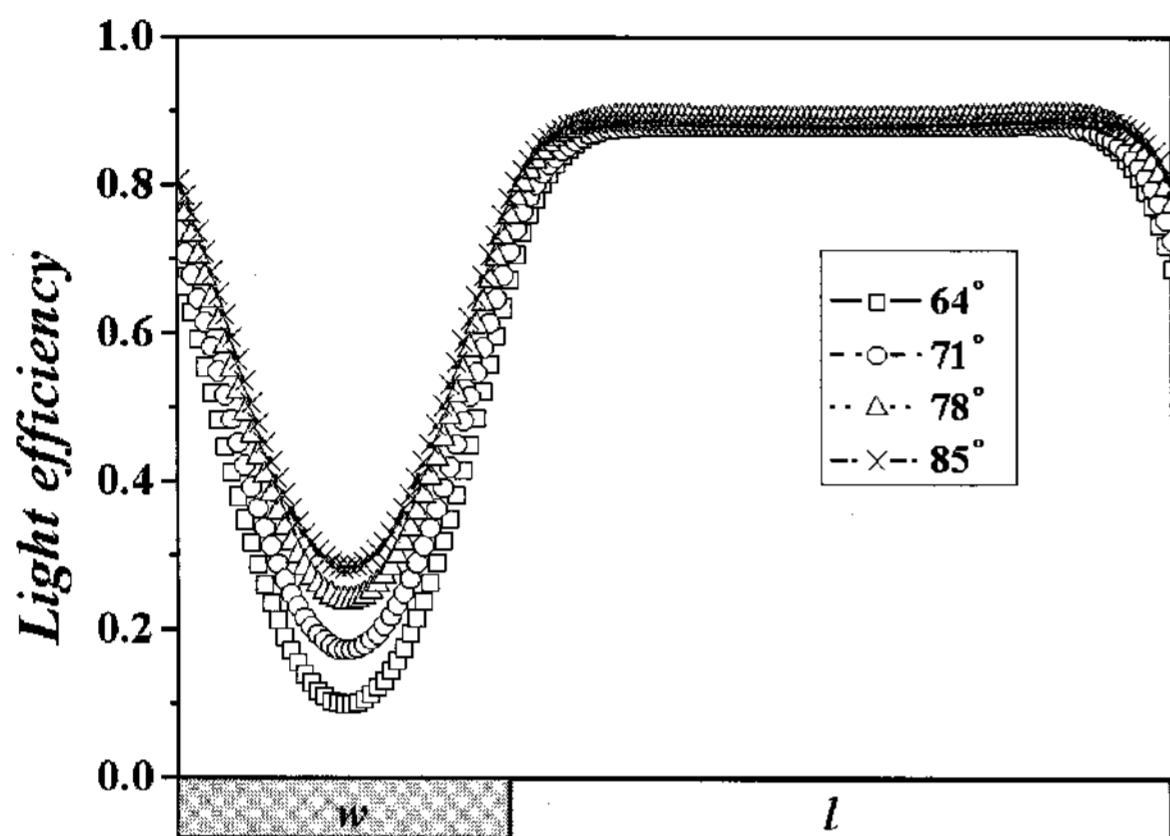


Fig. 3. Calculated light efficiency along the horizontal axis for different rubbing angles.

rubbing angle, when the operating voltage was applied, as shown in Fig. 4. At position *a* (near electrode edge), the twisted angle from the initial position is 43°, 44°, 45°, and 47° corresponding to the rubbing angles 64°, 71°, 78°, and 85° around $z/d = 0.32$, respectively. At position *b* (between the edge and the center of the electrode), the twisted angle from the initial position is 22°, 25°, 26°, and 29° corresponding to the rubbing angles 64°, 71°, 78°, and 85° around $z/d = 0.32$, respectively. At position *c* (at the center of the electrode), the twisted angle from the initial position is 12°, 15°, 18°, and 23° corresponding to the rubbing angles 64°, 71°, 78°, and 85° around $z/d = 0.32$, respectively.

Next, we calculated the average twist angle as a function of rubbing angle at three different positions, as shown in Fig. 5. As clearly shown in this figure, it is 15° for the 85° rubbed cell but only 5° for the 64° rubbed cell. This difference decreases rapidly as the electrode position approaches the electrode edge. From these results, we know that the increased transmittance in the 85° rubbed cell compared to the 64° rubbed cell is due to the difference in the twist angle above the electrodes.

Now, the question is why the twist angle

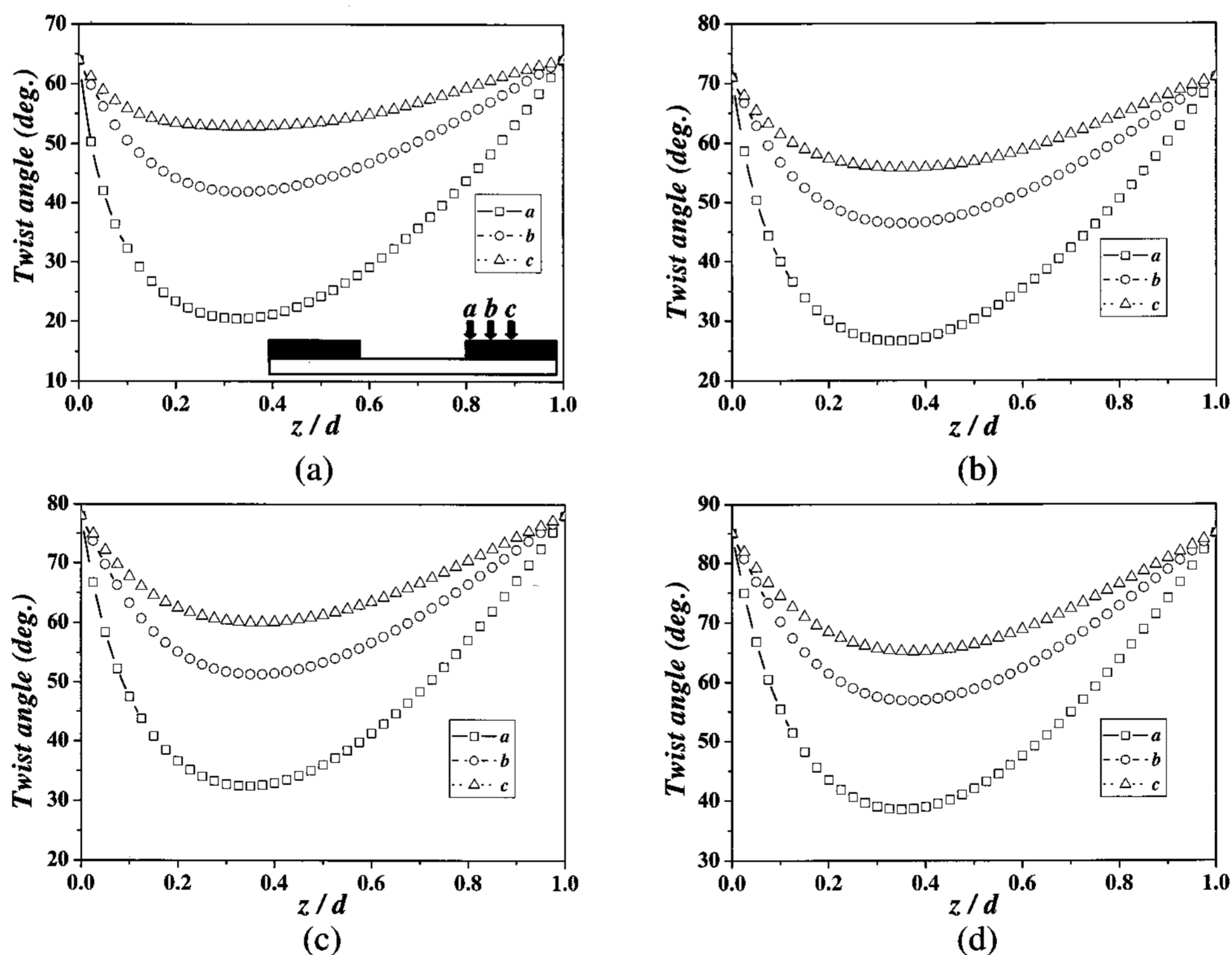


Fig. 4. Orientation of the twist angle for different rubbing angles at three different electrode positions: (a) 64°, (b) 71°, (c) 78°, and (d) 85°.

distribution show such a behavior. The first factor affecting the twist angle on the center of electrodes is the tilt angle at positions *a* and *b* since no horizontal field intensity exists at the center of electrodes and thus the LC twists only by twisting elastic force of the neighboring molecules. Therefore, we calculated the tilt angle at three different electrode positions along the vertical direction when the V_{op} was applied, as shown in Fig. 6. At position *c*, the

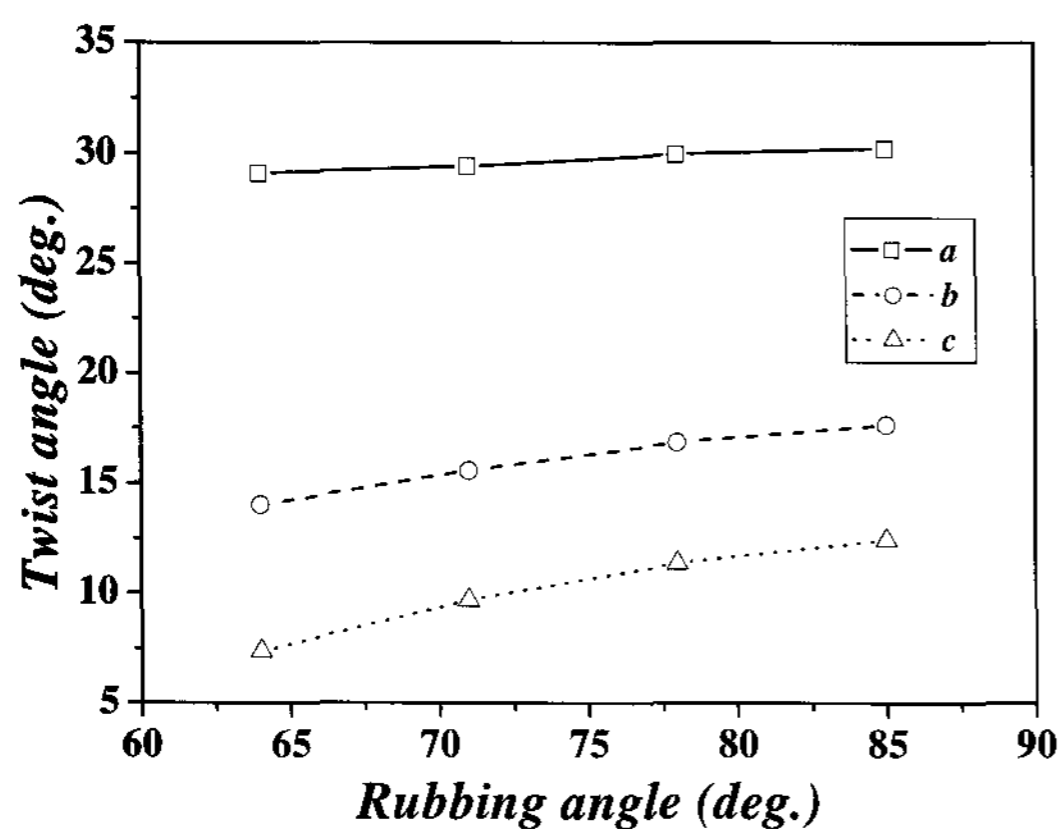


Fig. 5. Average twist angle for different rubbing angles at three different electrode positions.

initial tilt angle remained irrespective of the rubbing angles, however, at positions *a* and *b*, high tilt angles were generated and the degree of the tilt angle was strongly dependent on the vertical position and the rubbing angle. As can be seen from this figure, the maximal tilt angles at position *b* occurs around $z/d = 0.27$ and is -32° , -27° , -22° , and -19° (- sign indicates that the tilt angle is generated opposite to the initial tilting direction) for the rubbing angles 64° , 71° , 78° , and 85° , respectively. This difference correlates to the difference in the average twist angle at position *c*. For the generated LC's tilt angle to be large, the vertical electric field intensity at that position should be larger for the 64° rubbed cell than for the 85° rubbed cell.

First, the horizontal field intensity was calculated near the bottom surface and the middle of the cell for each differently rubbed cell, as shown in Fig. 7. At the edge of electrode, the field intensity was the strongest and increased as the rubbing decreased. This is attributed to the fact that the V_{op} is larger (5.8 V) for the 64° rubbed cell than that (4.8 V) for the 85° rubbed cell. Similarly, the vertical field intensity at positions *a* and *b* was much stronger for the 64° rubbed cell than for the 85° rubbed cell, as shown in Fig. 8. Based on the foregoing, we can conclude that the high

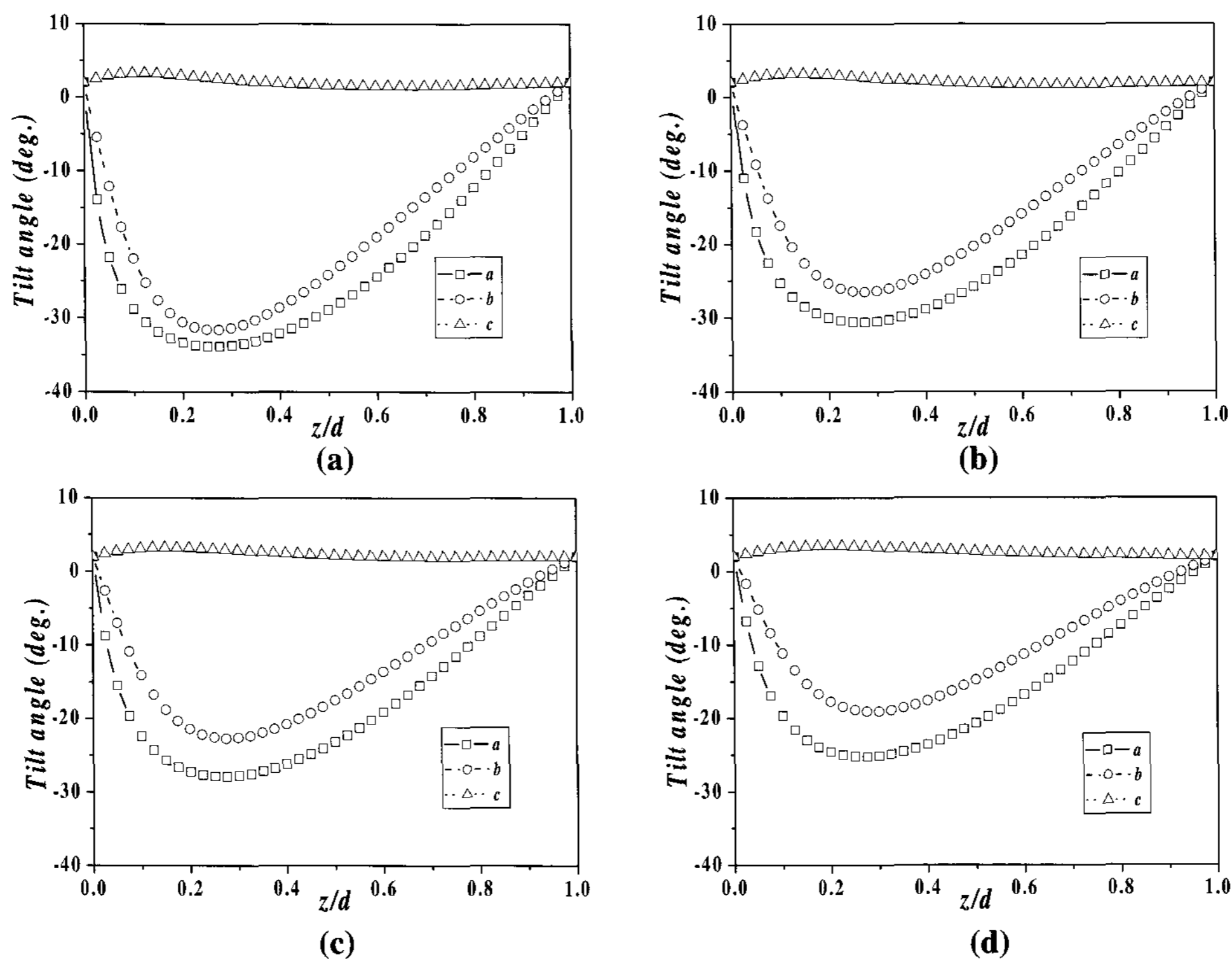


Fig. 6. Orientation of the tilt angle for different rubbing angles at three different electrode positions: (a) 64° , (b) 71° , (c) 78° , and (d) 85° .

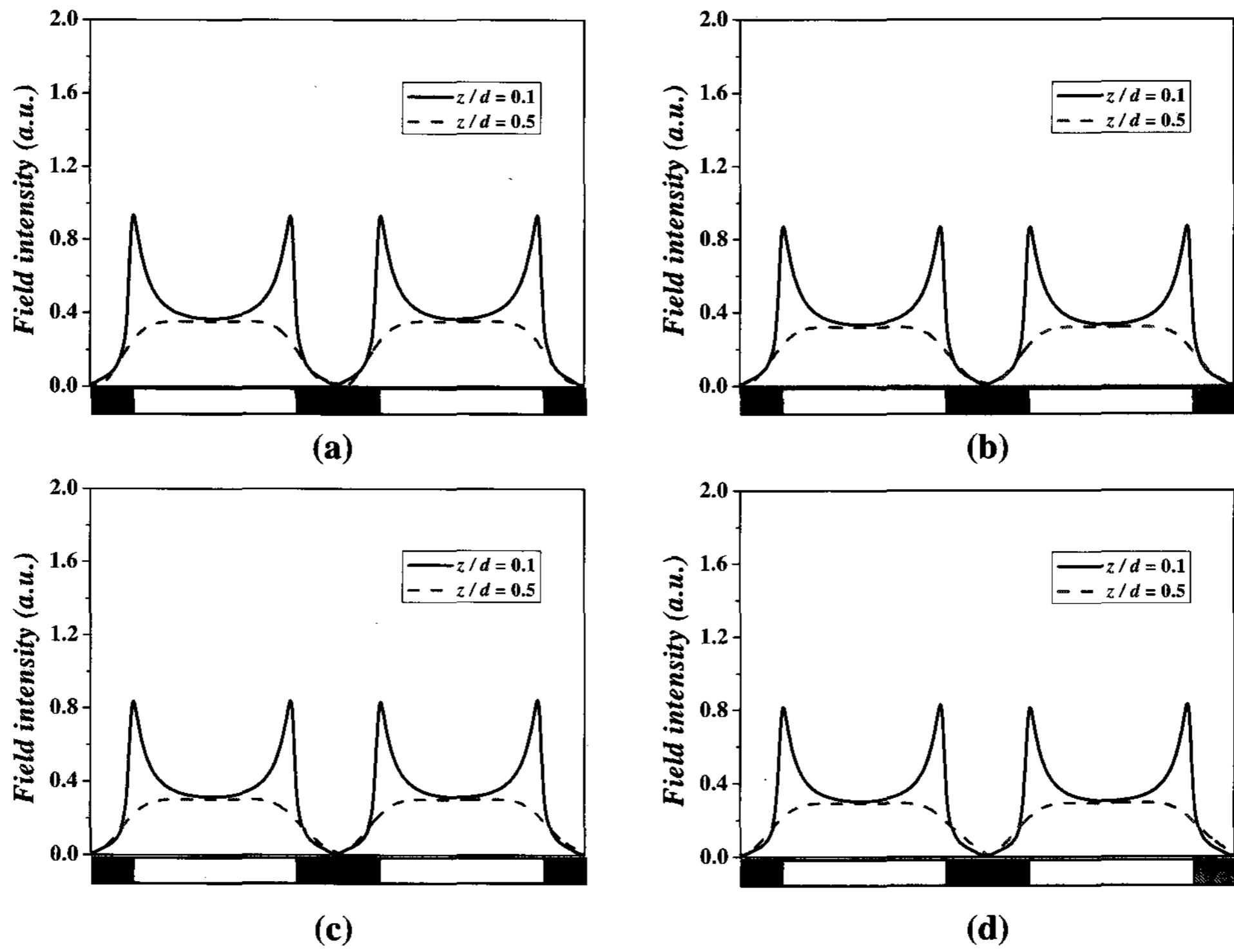


Fig. 7. Field distribution of the horizontal field intensity along the horizontal axis at $z/d = 0.1$ and 0.5 for different rubbing angles: (a) 64° , (b) 71° , (c) 78° , and (d) 85° .

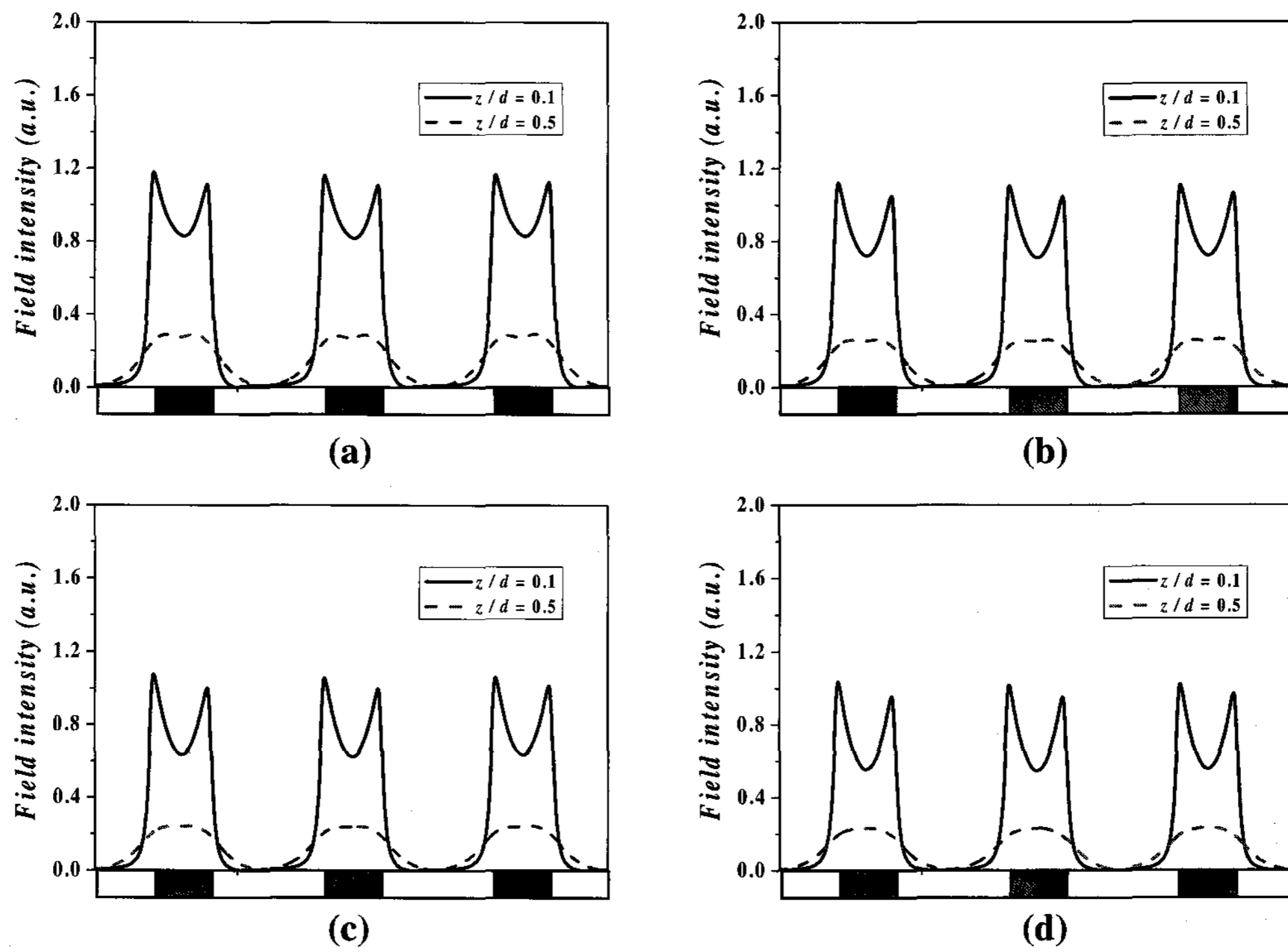


Fig. 8. Field distribution of the vertical field intensity along the horizontal axis at $z/d = 0.1$ and 0.5 for different rubbing directions: (a) 64° , (b) 71° , (c) 78° , and (d) 85° .

operating voltage in the 64° rubbed cell generates a stronger vertical field intensity than that in the 85° rubbed cell, and as a result, generating a high tilt angle at positions *a* and *b*. This in turns, results in lesser twist angle at position *c* for the 64° rubbed cell than that in the 85° rubbed cell.

To confirm these results, we fabricated the test cell under the same cell condition as in the simulation conditions and by using the LC ($\Delta n = 0.099$ at $\lambda = 589 \text{ nm}$, $\Delta \epsilon = 8.2$, $d = 3.2 \mu\text{m}$) and measured voltage-dependent trans-mission characteristics as shown in Fig. 9. As clearly shown in this figure, the 80° rubbed cell shows a lower driving voltage and higher transmittance than those of the 60° rubbed cell. Next, the light efficiency and the operational voltage were calculated as a function of w and l to clearly verify the relationship between them. Fig. 10 shows the calculated light efficiency and V_{op} dependent to w and l . The length of w and l part was varied to $3\sim 5 \mu\text{m}$

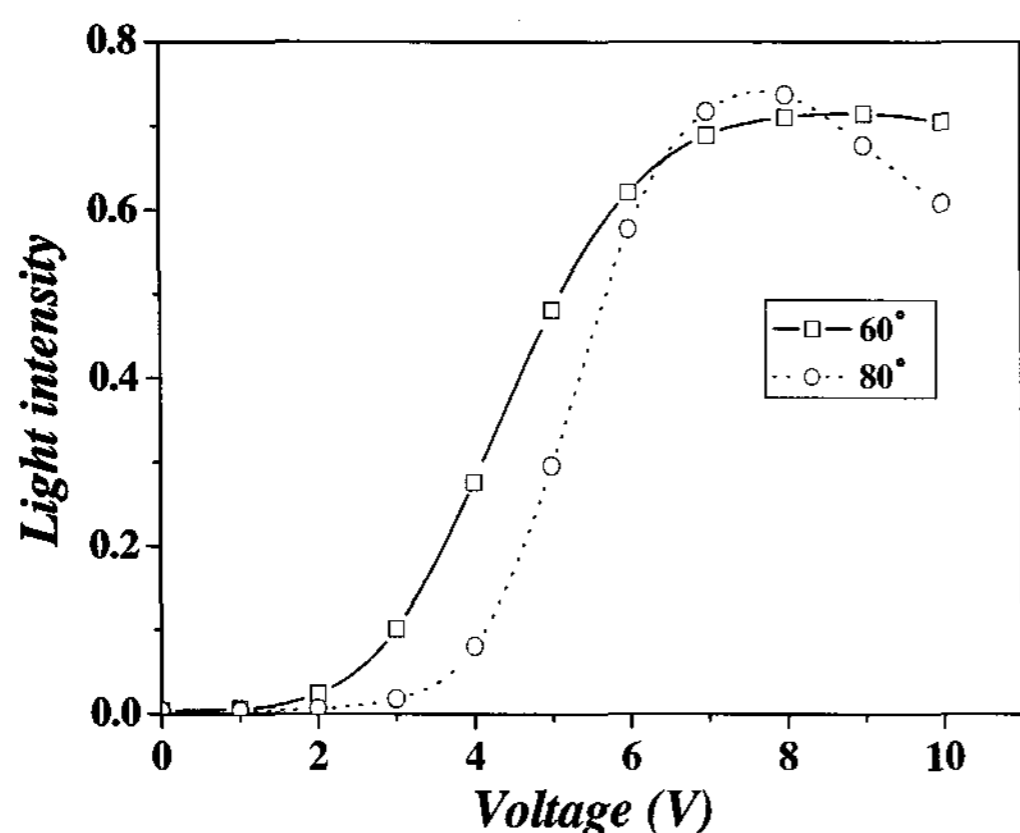


Fig. 9. Measured voltage-dependent transmittance for two different rubbing angles.

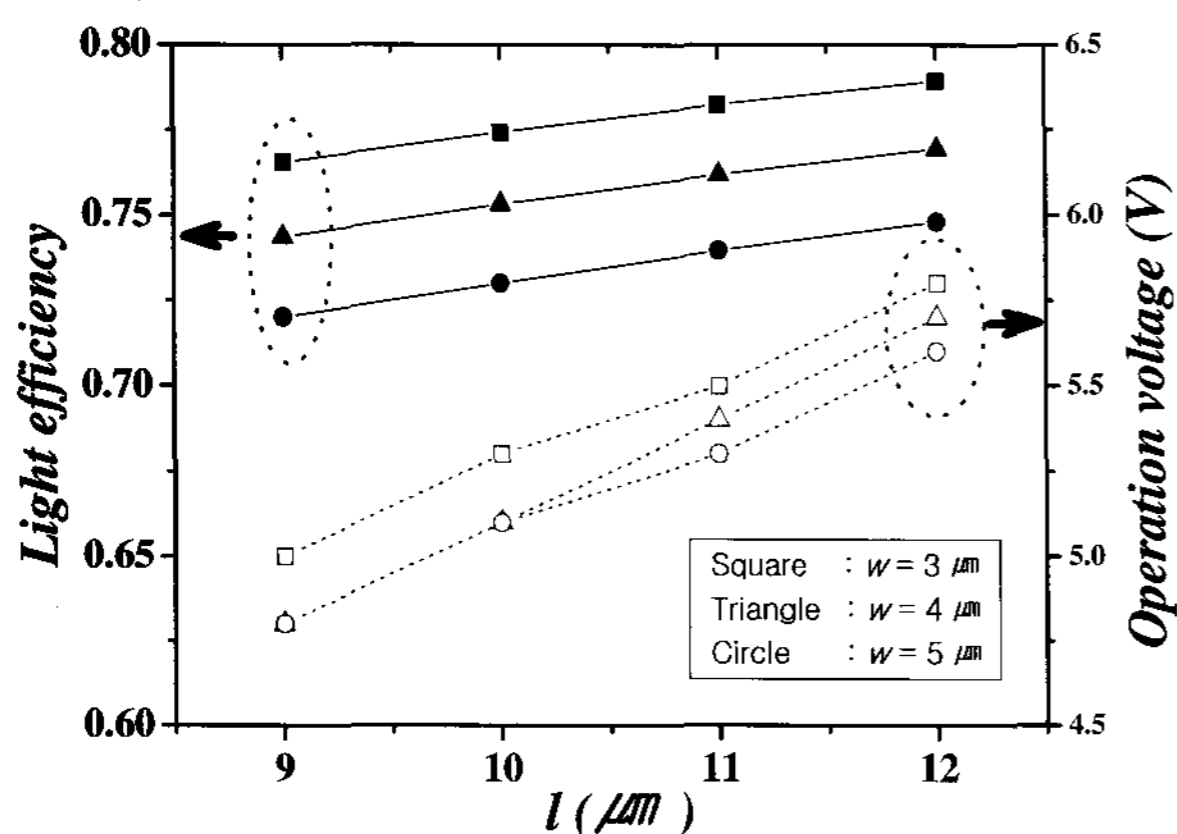
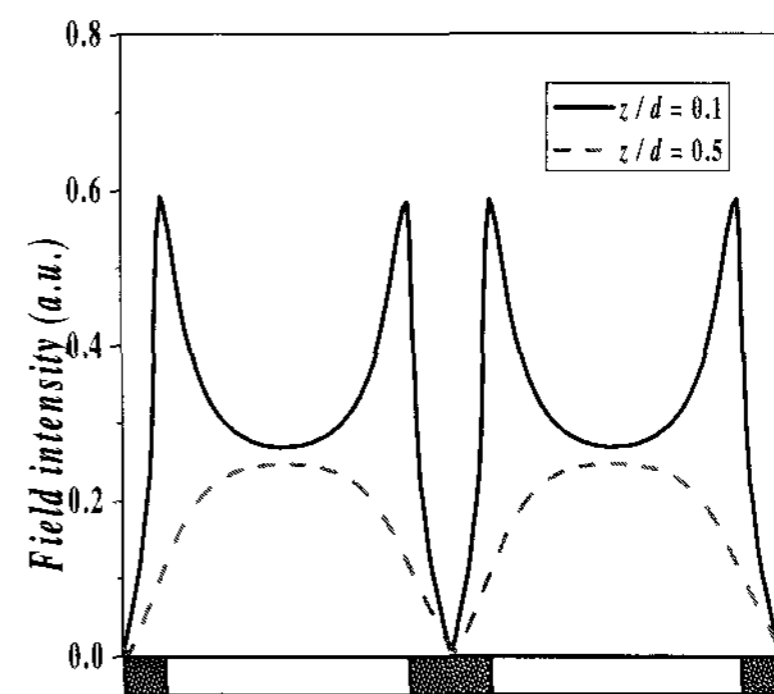
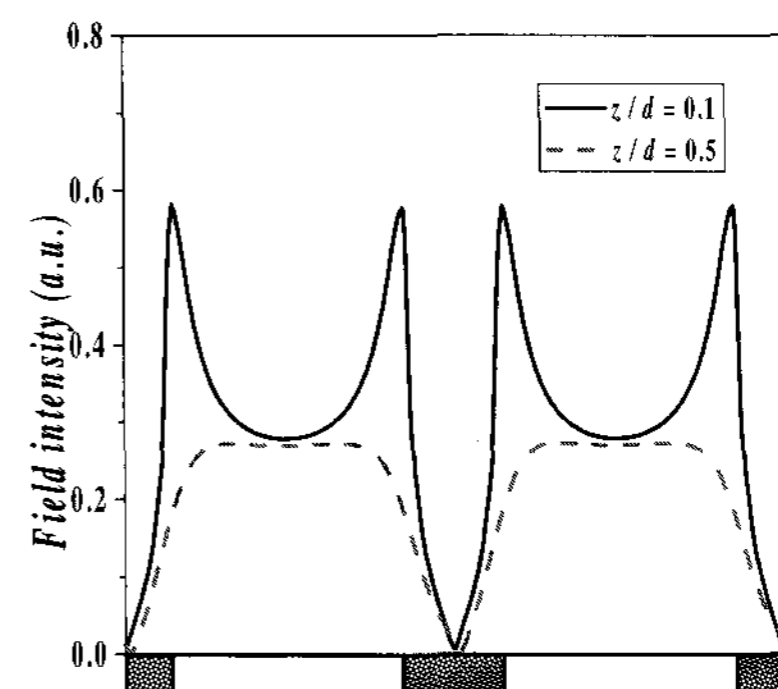


Fig. 10. Calculated light efficiency and V_{op} depending on w and l .

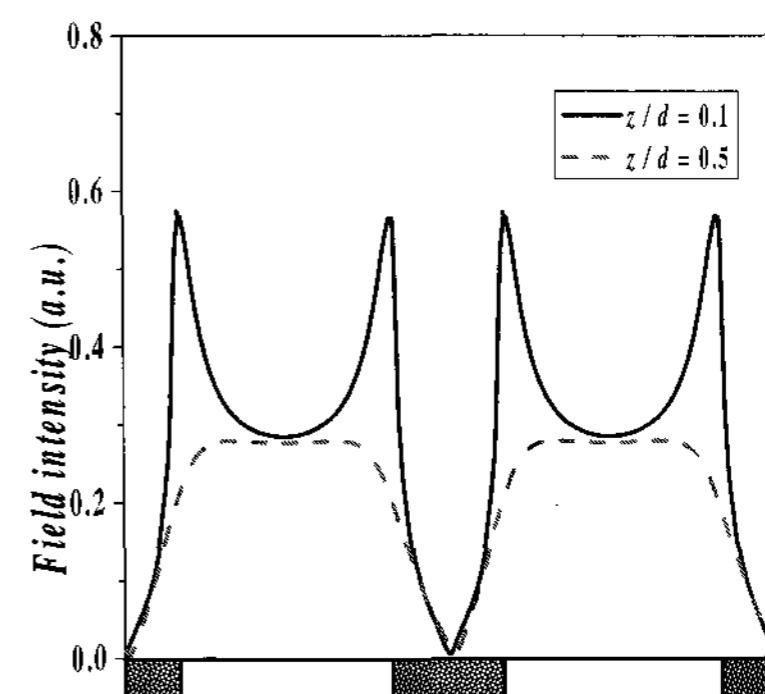
and $9\sim 12 \mu\text{m}$, respectively, while the rubbing angle was fixed as 80° with respect to the horizontal field ($d\Delta n$ is $0.32 \mu\text{m}$). As can be seen from this figure, as the l increases, the light efficiency is slightly improved irrespective of the w . However, the more the w increases, the lower light efficiency are achieved, due to increased equipotential area above the electrodes which generates reduced dielectric



(a)



(b)



(c)

Fig. 11. Horizontal field intensity with w at fixed l when the applied voltage is 5 V : (a) $w = 3 \mu\text{m}$, $l = 11 \mu\text{m}$ (b) $w = 4 \mu\text{m}$, $l = 11 \mu\text{m}$ and (c) $w = 5 \mu\text{m}$, $l = 11 \mu\text{m}$.

torque with increased w . Nevertheless, the driving voltage was found to decreased with increasing w and was also proportional to the l , as expected.

To understand why the larger w results in lower V_{op} , we calculated the horizontal field distribution at 5 V applied along electrodes at two different positions: near the bottom surface and at the middle of the cell, as shown in Fig. 11. In the IPS mode, the mid-director twists most with bias voltage so that the stronger the in-plane field, the LC director twists at lower voltage. The field distribution and intensity near the bottom surface is almost the same irrespective of the electrode width. However, one can see that at the middle of the cell, the in-plane field is stronger and more uniform field distribution in the cell with $w = 5 \mu\text{m}$ than those in the cell $w = 3 \mu\text{m}$.

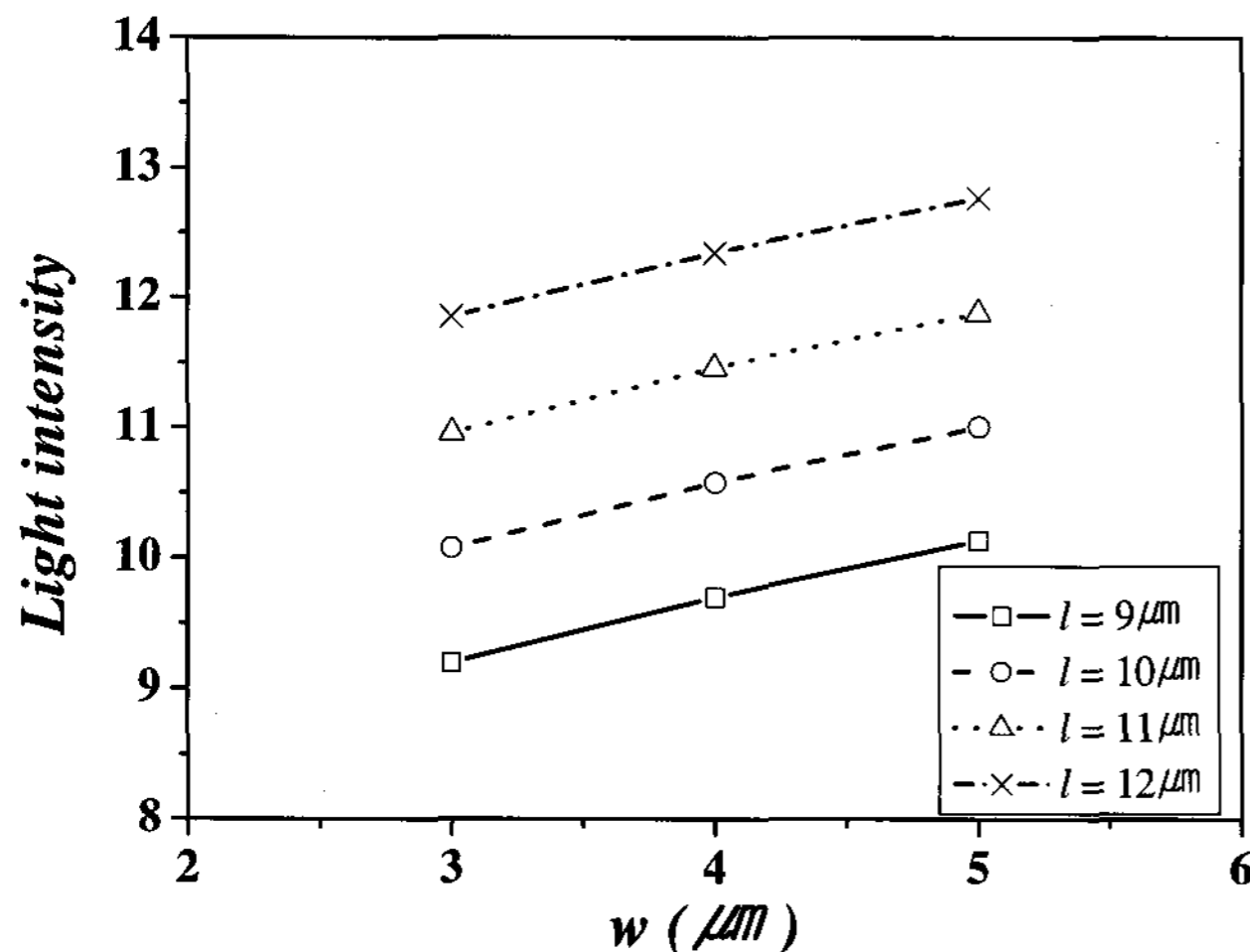


Fig. 12. The average light intensity with variation of w and l .

Finally, the light intensity was calculated as a function of w for each l , as shown in Fig. 12. Since the light intensity is linearly proportional to the l and w , the larger them it is increased. Nevertheless, the light intensity of the cell with $w = 5 \mu\text{m}$ and $l = 9 \mu\text{m}$ ($l = 11 \mu\text{m}$) was about the same as that of the cell with $w = 3 \mu\text{m}$ and $l = 10 \mu\text{m}$ ($l = 12 \mu\text{m}$), respectively. From the viewpoint of the V_{op} , the former was less than the latter. In designing a real pixel of the IPS mode, it would be sufficient if the space is 1 or 2

μm space so that if one wants the cell to have a low while exhibiting little change in the transmittance, the former condition is favorable.

4. Conclusion

In this study, we investigated the transmittance and the driving voltage as a function of the rubbing angle and electrode condition in an IPS mode, when both pixel and common electrodes are transparent. Unlike in the IPS mode that uses opaque electrodes, the light efficiency was dependent on the rubbing angle due to the different twist angles which in turn were dependent on the rubbing angles above the center of electrodes. Furthermore, to achieve a maximum light transmittance at low driving voltage, the electrode width and the distance between them need to be optimized such that the larger is the electrode width, the larger is the in-plane field intensity resulting in low driving voltage.

References

- [1] M. Schadt, and W. Helfrich, *Appl. Phys. Lett.* **18**, 127 (1971).
- [2] H. Yoshida, and J. Kelly, *Jpn. J. Appl. Phys.* **36**, 2116 (1997).
- [3] M. Oh-E, and K. Kondo, *Jpn. J. Appl. Phys.* **36**, 6798 (1997).
- [4] K. Kondo, S. Matsuyama, N. Konishi, and H. Kawakami, in *SID 98 Digest* (1998), p. 389.
- [5] S. H. Lee, S. L. Lee, and H. Y. Kim, in *Asia Display '98* (1998), p. 371.
- [6] S. H. Hong, I. C. Park, H. Y. Kim, and S. H. Lee, *Jpn. J. Appl. Phys.* **39**, L527 (2000).
- [7] S. H. Lee, H. Y. Kim, S. M. Lee, S. H. Hong, J. M. Kim, J. W. Koh, J. Y. Lee, and H. S. Park, in *SID 01 Digest* (2001), p. 117.
- [8] N. Koma, Y. Baba, and K. Matsuoka, in *SID 95 Digest* (1995), p. 869.
- [9] A. Lien, *Appl. Phys. Lett.* **57**, 2767 (1990).
- [10] H. Y. Kim, I. S. Song, and S. H. Lee, *Trans. on EEM.* **4**, 24 (2003).